Polymer Journal (2018) 50:737–743
https://doi.org/10.1038/s41428-018-0043-9

ORIGINAL ARTICLE

Cellular behaviors on polymeric scaffolds with 2D-patterned mechanical properties

Shinichiro Shimomura[1] · Hisao Matsuno[1,2] · Yohei Kinoshita[3] · Satoshi Fujimura[3] · Keiji Tanaka[1,2]

Received: 20 January 2018 / Revised: 24 February 2018 / Accepted: 27 February 2018 / Published online: 6 April 2018

Abstract

We propose a novel concept for cellular scaffolds with 2D-patterned mechanical properties. Thin films of glassy polystyrene (PS) with thicknesses ranging from 100 nm to 1 μm were prepared on epoxy resin-based line and space (L&S) patterned substrates. Although the outermost surface of PS on the L- and S-regions was sufficiently flat at the same level, the mechanical responses differed depending on the presence of the underlying resin foundation. The initial cell adhesion and spreading and the proliferation on the scaffolds were affected by the 2D-patterned mechanical properties, that is, cellular behavior was suppressed on mechanically unstable S-regions.

Introduction

Recently, in vitro cell culture devices made from synthetic polymers have attracted considerable attention [1–6]. Generally, adherent cells require suitable scaffolds [7–9] and physiologically active substances [10, 11] in a cell-culture environment to maintain their original functions. However, some external humoral factors may cause serious damage to cells [11–13]. Therefore, the regulation of cell functions [1, 6, 14–16] and the collection of cultured cells [17] by only tuning the structural and physical properties of polymeric scaffolds are important for further advances in the biotechnology and biomedical fields. A typical example of this is to prepare a cell sheet on the basis of the change in aggregation state of a thermoresponsive polymer in a scaffold [17, 18]. Poly(*N*-isopropylacrylamide) (PNIPAAm) starts to dissolve in water at ~305 K [19]. Thus, a layer of cultured cells on PNIPAAm can be gently detached by cooling them to this temperature, without the use of digestive enzymes or denaturing treatments. This technology contributes considerably to the regenerative medicine field combined with cell engineering using induced pluripotent stem (iPS) cells [20], resulting in the generation of various types of tissues from exfoliated cell sheets.

The physical properties, like the mechanical properties, of polymeric scaffolds are also one of the key factors regulating the functions of cells cultured on the scaffolds [1, 14–16, 21–27]. In most cases, the static elastic modulus of the polymeric scaffolds is set in the kPa range, mimicking a typical extra cellular matrix (ECM) [28, 29]. In addition, the temperature-responsive dynamic elastic change has also been used to control cellular functions [23]. Therein, the morphology of myoblasts on a cross-linked poly(ε-caprolactone) scaffold depended on the crystal-amorphous transition, ranging from a few MPa to several tens of MPa.

The mechanical properties not only in the bulk but also at the surface [30–32] play a key role in cell regulation. We recently studied the effect of surface mechanical properties on cellular phenomena for thin films made from typical glassy polymers of polystyrene (PS) [33] and poly(methyl methacrylate) (PMMA) [34]. The initial adhesion of L929 mouse fibroblasts on the films prepared on glass substrates was insensitive to the surface modulus, which ranged from GPa to MPa. However, in the case of bilayer scaffolds

✉ Hisao Matsuno
h-matsuno@cstf.kyushu-u.ac.jp

✉ Keiji Tanaka
k-tanaka@cstf.kyushu-u.ac.jp

[1] Department of Applied Chemistry, Kyushu University, Fukuoka 819-0395, Japan

[2] International Institute for Carbon-Neutral Energy Research (WPI-I2CNER), Kyushu University, Fukuoka 819-0395, Japan

[3] Tokyo Ohka Kogyo Co. Ltd., Kanagawa 211-0012, Japan

composed of glassy polymers on rubbery polyisoprene (PI), the cell adhesion and spreading were dependent on the thickness of the upper glassy layer if it became thinner than a threshold value [33, 34]. This finding could be explained in terms of the manifestation of the mechanical response from the underlying PI phase, called thinning-induced mechanical instability [33]. We further examined this issue using a film of poly[(2-methoxyethyl vinyl ether)-*block*-(L-lactic acid)] (P(MOVE-*b*-LLA)), in which the surface was covered with PMOVE [35], and found that fibroblasts were sufficiently sensitive to identify crystalline/non-crystalline regions of PLLA existing underneath the surface PMOVE layer. These results suggest that typical stiff polymers, unlike ECM, can be used as functional cellular scaffolds based on their surface mechanical properties. In this study, we propose a novel scaffold for the realization of patterned cellular behavior on a flat surface on the basis of the mechanical instability of synthetic glassy polymers. This novel methodology for cell patterning enables the potential development of further-functionalized arrays of living cells, which are applicable to cell-based sensors and drug discovery devices in the biomedical field [36, 37].

Experimental

Scaffold preparation

PS with a number-average molecular weight (M_n) of 235k and a molecular weight distribution (M_w/M_n) of 1.05, where M_w is the weight-average molecular weight, was purchased from Polymer Source Inc. (Dorval, QC, Canada). Figure 1 shows the preparation process for a cellular scaffold with 2D-patterned mechanical properties. A spin-coated PS film on a silicon wafer was removed from the wafer and then floated to the surface of ultrapure water purified by a Milli-Q system (Merck KGaA, Darmstadt, Germany) [38]. The thickness of the PS film (d_{PS}) was adjusted from 100 nm to 1 µm. Then, the film was transferred onto an epoxy resin-based line and space (L&S) pattern substrate prepared by photolithography (Tokyo Ohka Kogyo Co. Ltd., Kanagawa, Japan). The height difference and half pitch of the L&S pattern were 2.4 and 40 µm, respectively. The PS/L&S scaffold was dried at a room temperature of approximately 298 K for 24 h under vacuum. The morphology of the L&S patterned substrate before and after the transfer of the PS

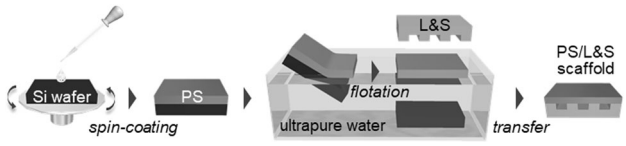

Fig. 1 A schematic illustration of the preparation of a PS/L&S scaffold

film was examined by using a LEXT OLS4000 3D laser measuring microscope (Olympus Co., Tokyo, Japan). In addition, sectional views of the scaffold were observed by scanning electron microscopy (SEM, SS-550, Shimadzu Co., Kyoto, Japan).

Cell culturing

Suspensions of mouse fibroblast L929 cells (Cell Engineering Division, RIKEN BioResource Center, Tsukuba, Japan) at 5.0×10^4 cells/well were seeded onto the PS/L&S scaffolds placed on the base of 24-well culture dishes filled with cell culture medium, normal Roswell Park Memorial Institute (RPMI) 1640 medium (Life Technologies Japan Ltd., Tokyo, Japan), with/without 10% fetal bovine serum (FBS, Life Technologies Japan). The cultures were maintained at 310 K (37 °C) in a humidified atmosphere containing 5% CO_2. After 4 h of culturing, the scaffold surfaces were rinsed to remove cells floating in the culture medium. The number and morphology of cells on the PS/L&S scaffolds at a given culturing time were evaluated by phase contrast microscopy (BZ-8100, Keyence Co., Osaka, Japan). Additionally, cell proliferation under serum conditions was observed as a function of the culturing time in the same manner. The projected area of cells was quantified by using ImageJ software (National Institutes of Health, USA).

Results and discussion

Scaffold morphology

Figure 2a, b shows 3D-confocal laser scanning microscopic (CLSM) images of the L&S patterned substrate before and after picking up a 100 nm-thick PS film. Although the film was very thin, the top surface was quite flat without any defects, as shown in Fig. 2b. Figure 2c, d shows sectional views of the L&S patterned substrate before and after the transfer of the 100 nm-thick PS film observed by SEM. As mentioned above, the manifestation of thinning-induced mechanical instability for thin polymer films is strongly dependent on the underlying region [32]. Considering that the underlying region of the PS film is composed of either the epoxy resin with an elastic modulus of 3.0 GPa or air, hereafter referred to as the L- or S-regions, respectively, it can be posited that this scaffold possesses 2D-patterned mechanical properties.

Cell adhesion under serum-free conditions

First, cell culturing on the PS/L&S scaffold was performed under serum-free conditions, that is, the integrin-independent interaction between the cells and polymer

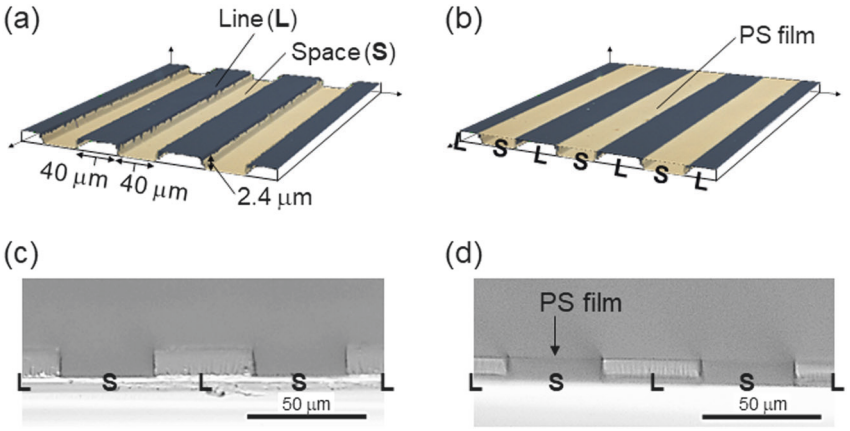

Fig. 2 **a**, **b** 3D-CLSM images of the L&S patterned substrate **a** before and **b** after the transfer of a 100 nm-thick PS film. The half pitch of the L&S patterned substrate was 40 μm, and the widths of the L- and S-regions were the same. The height difference between the L- and S-regions was 2.4 μm. **c**, **d** Sectional views of the L&S patterned substrate from SEM **c** before and **d** after the transfer of the thin PS film

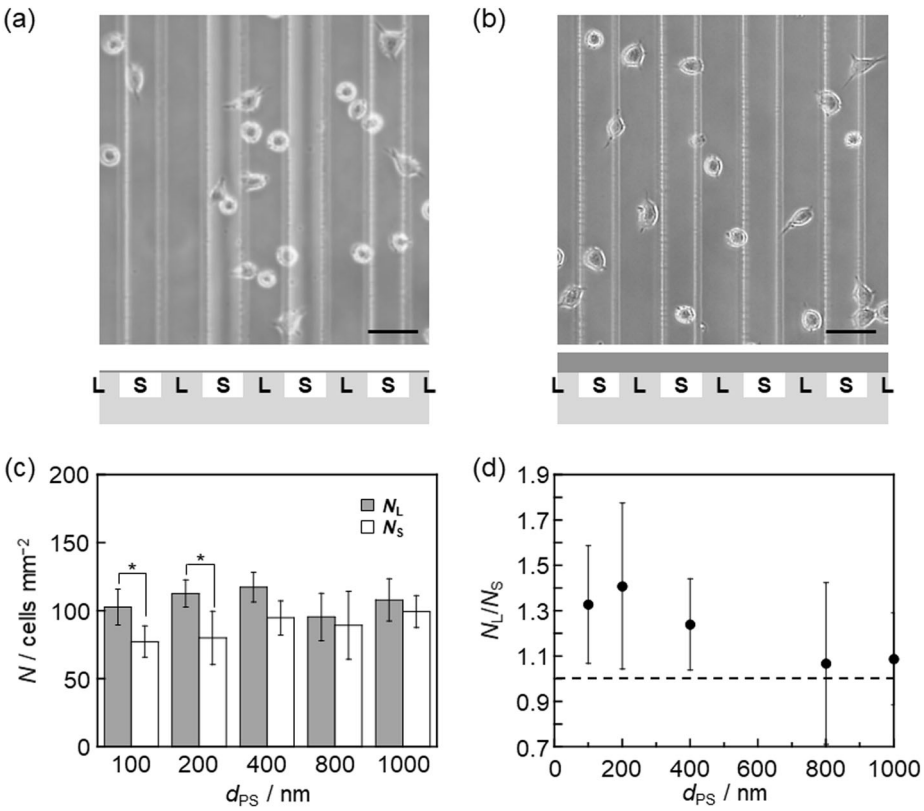

Fig. 3 Phase-contrast images of L929 fibroblasts attached to the PS/L&S scaffolds with d_{PS} values of **a** 100 nm and **b** 1 μm, respectively, under serum-free conditions. Scale bars correspond to 50 μm. Schematic illustrations of the scaffolds accompany the images. **c** The number of cells adhered on the L- and S-regions (N_L and N_S). Data are the mean values with standard deviations. $*p < 0.05$ (Student's *t*-test). **d** The d_{PS} dependence of the ratio of mean N_L to mean N_S values (N_L/N_S)

scaffolds was examined [39–41]. Figure 3a, b shows the phase-contrast images of L929 cells cultured on the PS/L&S scaffolds with different d_{PS} values for 4 h. Although the dividing lines between the L- and S-regions can be discerned in the images, the scaffold geometry is also shown for easy understanding. While the cell adhesion on the 1 μm-thick PS scaffold was homogeneous over the 2D mechanical pattern, as shown in Fig. 3b, more cells were attached to the L-regions than to the S-regions of the 100 nm-thick PS scaffold, as shown in Fig. 3a. Figure 3c shows the d_{PS} dependence of the number of cells adhered on the L- and S-regions (N_L and N_S), and the ratio of the mean N_L to mean N_S values is shown in Fig. 3d. When the PS film was thicker than 800 nm, the ratio was independent of the underlying L&S pattern. On the other hand, when the d_{PS} fell short of 400 nm, N_L was greater than N_S, and their difference showed a tendency to increase with decreasing d_{PS}. These points make it clear that L929 cells can recognize the 2D mechanical pattern of the scaffolds.

Figure 4a, b shows the projected area of cells attached to the PS/L&S scaffolds with d_{PS} values of 100 nm and 1 μm, respectively. The peak position and full width at half maximum (FWHM) obtained from the normal distribution curves are summarized in Table 1. While the cell spreading

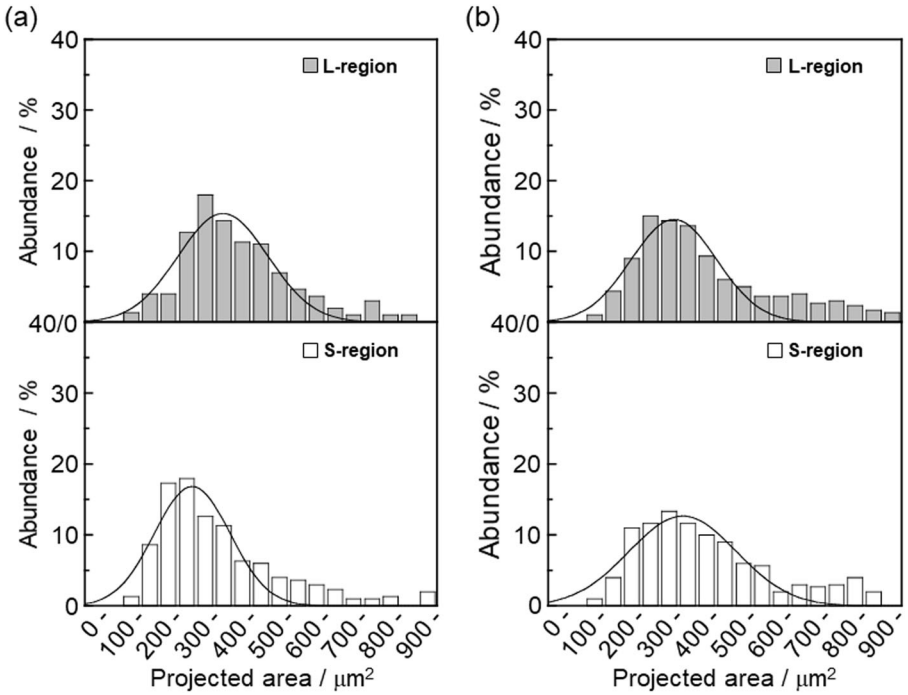

Fig. 4 The abundance of the projected area of cells adhered on the L- and S-regions for scaffolds with d_{PS} values of **a** 100 nm and **b** 1 μm. Normal distribution curves are superimposed for reference

Table 1 Peak position and full width at half maximum (FWHM) with the standard deviation for the normal distribution curves in Fig. 4

d_{PS} (nm)	Region	Peak position (μm^2)	FWHM (μm^2)
100	L	398 ± 10	286 ± 23
100	S	315 ± 11	240 ± 25
1000	L	363 ± 12	271 ± 27
1000	S	387 ± 14	339 ± 33

was not dependent on the underlying L&S pattern for the thicker PS scaffolds, cells attached onto the L-regions of the thinner scaffolds spread well in comparison with those attached to the S-regions. Thus, these results demonstrate again that the cell adhesion and spreading at the initial stage under serum-free conditions was somehow controlled by the L&S pattern if the upper PS film was sufficiently thin.

Cell adhesion and proliferation under serum conditions

Second, cellular behaviors were monitored for a longer time under serum conditions to examine the impact of surface mechanical properties on cell proliferation as well as adhesion [11]. Figure 5 shows the phase-contrast images of L929 fibroblasts cultured on the PS/L&S scaffolds with different d_{PS} values for (a, b) 4 h and (c, d) 72 h. In the case of the 4 h cell culture, while the cell adhesion was not dependent on the 2D mechanical pattern for the 1 μm-thick PS scaffold, it was slightly dependent for the 100 nm-thick PS one. This trend became clear after 72 h, as shown in Fig. 5c, d. Figure 5e, f shows the number of cells adhered to the L- and S-regions after 4 h and 72 h of culture, respectively. Figure 5g shows the culturing time dependence of N_L/N_S. In the case of 4 h, the N_L/N_S ratio was almost unity for the scaffolds with a PS layer thicker than 800 nm and was slightly higher for the scaffolds with a thinner PS layer. This cell adhesion behavior at the initial stage was similar to that observed under serum-free conditions. When the culturing time increased to a few days for the scaffolds with a PS layer thicker than 800 nm, both N_L and N_S increased to the same amount, that is, L929 cells uniformly attached to and proliferated on the scaffold surface. Conversely, when the upper PS layer became thinner than 400 nm, N_L was clearly greater than N_S, and this difference became more remarkable as the culturing time increased. These points make it clear that fibroblast proliferation and migration as well as adhesion could be regulated by the 2D mechanical pattern of the scaffold.

It has been reported that integrin-mediated cell adhesion causes conformational changes in mechanosensitive proteins owing to the induced tension, which are involved in changing the connections between the ECM and actin cytoskeleton, so-called actin remodeling [42–45]. As a consequence, the signal transduction pathway is activated to alter cellular behaviors such as proliferation and migration. Taking this into account, a possible explanation for the cellular behaviors observed here is that the difference in the mechanical response between the S- and L-regions of the

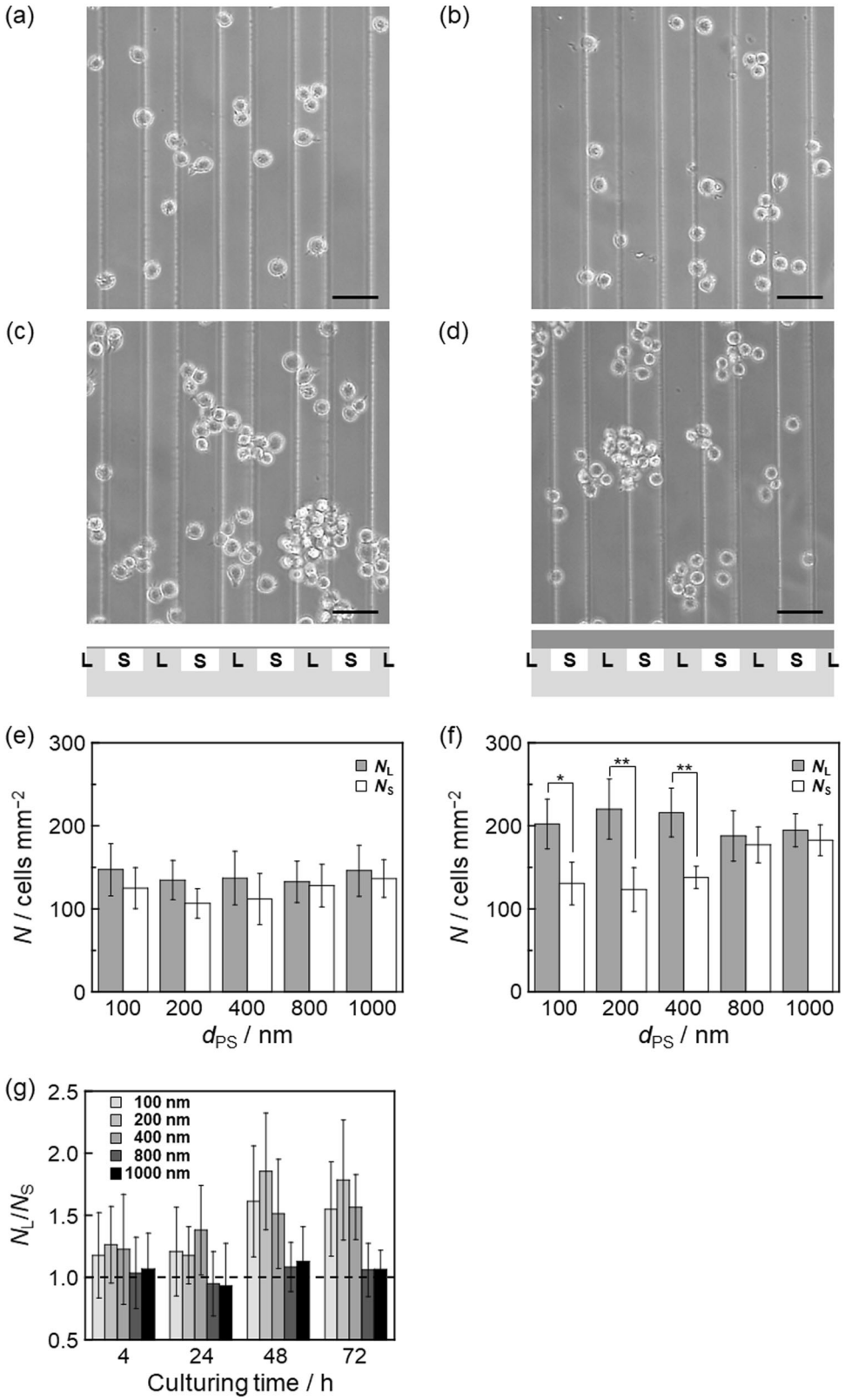

Fig. 5 Phase contrast images of L929 fibroblasts attached to the PS/L&S scaffolds with d_{PS} values of **a**, **c** 100 nm and **b**, **d** 1 μm cultured for **a**, **b** 4 h and **c**, **d** 72 h, respectively, in medium containing 10% FBS. Scale bars correspond to 50 μm. **e**, **f** The d_{PS} dependence of the number (N) of cells adhered on the L- and S-regions (N_S and N_L) for a culturing time of **e** 4 h and **f** 72 h, respectively. Data are the mean values with standard deviations. $*p < 0.05$; $**p < 0.005$ (Student's t-test). **g** Culturing time dependence of N_L/N_S

scaffold could lead to a different level of activation for actin remodeling on these regions. Another possible explanation is the gentle oscillation of the PS thin film on the S-region, which is always in contact with the culture medium. This oscillation does not occur on the L-region due to the foundation of the epoxy resin. Such a situation may also

contribute to the different level of activation for actin remodeling. A more conclusive study of this issue with finite element analysis is currently underway.

Conclusions

A novel concept for cellular scaffolds with 2D-patterned mechanical properties is proposed. Initial cell adhesion and spreading under serum-free conditions on the PS/L&S scaffold were suppressed on the S-regions compared to those on the L-regions once the upper PS film became thinner than a threshold value. In addition, under serum conditions, cell adhesion and proliferation were affected by the underlying L&S pattern with a thinner PS layer. Cellular behaviors on scaffolds composed of a common glassy polymer can be regulated on the basis of the physical properties of the scaffold, especially near the outermost region. We believe that this novel concept of cellular scaffolds will lead to the development of highly functional cellular scaffolds composed of synthetic polymers.

Acknowledgements This research was partly supported by JSPS KAKENHI, Grant-in-Aid for Scientific Research (A) (No. JP15H02183) to KT and for Scientific Research (C) (JP15K05633) to HM. We are also grateful for support from the Development of Advanced Measurement and Analysis System Program (JST-SENTAN) (13A0004) by the Japan Science and Technology Agency (JST) to KT and Impulsing Paradigm Change through Disruptive Technologies Program (ImPACT) by the Cabinet Office, Government of Japan, to KT.

Compliance with ethical standards

Conflict of interest The authors declare that they have no conflict of interest.

References

1. Engler AJ, Sen S, Sweeney HL, Discher DE. Matrix elasticity directs stem cell lineage specification. Cell. 2006;126:677–89.
2. Miyasako H, Yamamoto K, Aoyagi T. Preparation, characterization and biocompatibility study of the scaffold prototype derived from cross-linked poly[(ε-caprolactone)-*co*-lactide] for tissue engineering materials. Polym J. 2008;40:806–12.
3. Sawada T, Tsuchiya M, Takahashi T, Tsutsumi H, Mihara H. Cell-adhesive hydrogels composed of peptide nanofibers responsive to biological ions. Polym J. 2012;44:651–7.
4. Matsusaki M, Akashi M. Control of extracellular microenvironments using polymer/protein nanofilms for the development of three-dimensional human tissue chips. Polym J. 2014;46:524–36.
5. Fukushima K. Biodegradable functional biomaterials exploiting substituted trimethylene carbonates and organocatalytic transesterification. Polym J. 2016;48:1103–14.
6. Matsuno H, Matsuyama R, Yamamoto A, Tanaka K. Enhanced cellular affinity for poly(lactic acid) surfaces modified with titanium oxide. Polym J. 2015;47:505–12.
7. Langer R, Vacanti JP. Tissue engineering. Science. 1993;260:920–6.
8. Wong JY, Leach JB, Brown XQ. Balance of chemistry, topography, and mechanics at the cell–biomaterial interface: Issues and challenges for assessing the role of substrate mechanics on cell response. Surf Sci. 2004;570:119–33.
9. Discher DE, Mooney DJ, Zandstra PW. Growth factors, matrices, and forces combine and control stem cells. Science. 2009;324:1673–7.
10. Dubiel EA, Martin Y, Vermette P. Bridging the gap between physicochemistry and interpretation prevalent in cell-surface interactions. Chem Rev. 2011;111:2900–36.
11. Yao T, Asayama Y. Animal-cell culture media: History, characteristics, and current issues. Reprod Med Biol. 2017;16:99–117.
12. Delcroix GJ, Curtis KM, Schiller PC, Montero-Menei CN. EGF and bFGF pre-treatment enhances neural specification and the response to neuronal commitment of MIAMI cells. Differentiation. 2010;80:213–27.
13. Huang Z, Ren PG, Ma T, Smith RL, Goodman SB. Modulating osteogenesis of mesenchymal stem cells by modifying growth factor availability. Cytokine. 2010;51:305–10.
14. Vogel V, Sheetz M. Local force and geometry sensing regulate cell functions. Nat Rev Mol Cell Biol. 2006;7:265–75.
15. Hörning M, Kidoaki S, Kawano T, Yoshikawa K. Rigidity matching between cells and the extracellular matrix leads to the stabilization of cardiac conduction. Biophys J. 2012;102:379–87.
16. DeForest CA, Tirrell DA. A photoreversible protein-patterning approach for guiding stem cell fate in three-dimensional gels. Nat Mater. 2015;14:523–31.
17. Okano T, Yamada N, Okuhara M, Sakai H, Sakurai Y. Mechanism of cell detachment from temperature-modulated, hydrophilic-hydrophobic polymer surfaces. Biomaterials. 1995;16:297–303.
18. Natalia B, Henry A, Betty L, Marina RL, Roberto R. Probing poly (N-isopropylacrylamide-co-butylacrylate)/cell interactions by atomic force microscopy. J Biomed Mater Res A. 2015;103:145–53.
19. Heskins M, Guillent JE. Solution properties of poly(N-isopropylacrylamide). J Macromol Sci Chem A. 1968;2:1441–55.
20. Okita K, Ichisaka T, Yamanaka S. Generation of germline-competent induced pluripotent stem cells. Nature. 2007;448:313–7.
21. Discher DE, Janmey P, Wang YL. Tissue cells feel and respond to the stiffness of their substrate. Science. 2005;310:1139–43.
22. Yoshikawa HY, Rossetti FF, Kaufmann S, Kaindl T, Madsen J, Engel U, Lewis AL, Armes SP, Tanaka M. Quantitative evaluation of mechanosensing of cells on dynamically tunable hydrogels. J Am Chem Soc. 2011;133:1367–74.
23. Uto K, Ebara M, Aoyagi T. Temperature-responsive poly(ε-caprolactone) cell culture platform with dynamically tunable nano-roughness and elasticity for control of myoblast morphology. Int J Mol Sci. 2014;15:1511–24.
24. Fujie T. Development of free-standing polymer nanosheets for advanced medical and health-care applications. Polym J. 2016;48:733–80.
25. Navarro L, Ceaglio N, Rintoul I. Structure and properties of biocompatible poly(glycerol adipate) elastomers modified with ethylene glycol. Polym J. 2017;49:625–32.
26. Iijima K, Tsuji Y, Kuriki I, Kakimoto A, Nikaido Y, Ninomiya R, Iyoda T, Fukai F, Hashizume M. Control of cell adhesion and proliferation utilizing polysaccharide composite film scaffolds. Colloids Surf B Biointerfaces. 2017;160:228–37.
27. Shimomura S, Matsuno H, Ohta T, Kawahara S, Tanaka K. Initial adhesion of fibroblasts on thin rubber scaffolds. Chem Lett. 2016;45:475–7.
28. Meredith JE Jr., Fazeli B, Schwartz MA. The extracellular matrix as a cell survival factor. Mol Biol Cell. 1993;4:953–61.

29. Geiger B, Bershadsky A, Pankov R, Yamada KM. Transmembrane crosstalk between the extracellular matrix and the cytoskeleton. Nat Rev Mol Cell Biol. 2001;2:793–805.
30. Tanaka K, Takahara A, Kajiyama T. Rheological analysis of surface relaxation process of monodisperse polystyrene films. Macromolecules. 2000;33:7588–93.
31. Tanaka K, Taura A, Ge S, Takahara A, Kajiyama T. Molecular weight dependence of surface dynamic viscoelastic properties for the monodisperse polystyrene film. Macromolecules. 1996;29:3040–42.
32. Satomi N, Tanaka K, Takahara A, Kajiyama T. Effect of internal bulk phase on surface viscoelastic properties by scanning probe microscopy. Macromolecules. 2001;34:6420–3.
33. Shimomura S, Matsuno H, Tanaka K. Effect of mechanical instability of polymer scaffolds on cell adhesion. Langmuir. 2013;29:11087–92.
34. Shimomura S, Matsuno H, Sanada K, Tanaka K. Cell adhesion on glassy scaffolds with a different mechanical response. J Mater Chem B. 2017;5:714–9.
35. Matsuno H, Irie S, Hirata T, Matsuyama R, Oda Y, Masunaga H, Seki Y, Aoshima S, Tanaka K. Heterogeneous adhesion of cells on polymer surfaces with underlying amorphous/crystalline phases. J Mater Chem B. 2018;6:903–7.
36. Falconnet D, Csucs G, Grandin HM, Textor M. Surface engineering approaches to micropattern surfaces for cell-based assays. Biomaterials. 2006;27:3044–63.
37. Jung DR, Kapur R, Adams T, Giuliano KA, Mrksich M, Craighead HG, Taylor DL. Topographical and physicochemical modification of material surface to enable patterning of living cells. Crit Rev Biotechnol. 2001;21:111–54.
38. Kawaguchi D, Tanaka K, Takahara A, Kajiyama T. Surface mobile layer of polystyrene film below bulk glass transition temperature. Macromolecules. 2001;34:6164–6.
39. Serizawa T, Yamashita K, Akashi M. Cell-adhesive and blood-coagulant properties of ultrathin poly(methyl methacrylate) stereocomplex films. J Biomater Sci Polym Ed. 2004;15:511–26.
40. Hoshiba T, Nagahara H, Cho C-S, Tagawa Y, Akaike T. Primary hepatocyte survival on non-integrin-recognizable matrices without the activation of Akt signaling. Biomaterials. 2007;28:1093–104.
41. Hoshiba T, Yoshihiro A, Tanaka M. Evaluation of initial cell adhesion on poly (2-methoxyethyl acrylate) (PMEA) analogous polymers. J Biomater Sci Polym Ed. 2017;28:986–99.
42. Lin CH, Forscher P. Cytoskeletal remodeling during growth cone-target interactions. J Cell Biol. 1993;121:1369–83.
43. Stossel TP, Fenteany G, Hartwig JH. Cell surface actin remodeling. J Cell Sci. 2006;119:3261–4.
44. Tricheta L, Le Digabel J, Hawkins RJ, Vedula SR, Gupta M, Ribrault C, Hersen P, Voituriez R, Ladoux B. Evidence of a large-scale mechanosensing mechanism for cellular adaptation to substrate stiffness. Proc Natl Acad Sci USA. 2012;109:6933–8.
45. Prager-Khoutorsky M, Lichtenstein A, Krishnan R, Rajendran K, Mayo A, Kam Z, Geiger B, Bershadsky AD. Fibroblast polarization is a matrix-rigidity-dependent process controlled by focal adhesion mechanosensing. Nat Cell Biol. 2011;13:1457–65.